NUMERICAL STUDY OF VORTICAL STRUCTURES AROUND A WALL-MOUNTED CUBIC OBSTACLE IN CHANNEL FLOW, USING THE IMMERSED BOUNDARY METHOD

João Marcelo Vedovoto, jmvedovoto@mecanica.ufu.br
School of Mechanical Engineering - Federal University of Uberlândia João Naves de Ávila Av. 2121,Uberlândia, MG, Brazil

Rubens Campregher, rubenscamp@dal.ca
Department of Mechanical Engineering - Dalhousie University A1B 3X5 - Halifax, NS - Canada

Aristeu da Silveira Neto, aristeus@mecanica.ufu.br
School of Mechanical Engineering - Federal University of Uberlândia João Naves de Ávila Av. 2121,Uberlândia, MG, Brazil

Abstract. *The mathematical modeling and the numerical simulation of practical engineering problems involving flow around bodies are receiving increasing attention lately. Nonetheless, accurate and viable algorithms still constitute great challenge to researchers. This paper aims to present an in-house Immersed Boundary (IB) methodology for modeling flows over complex three-dimensional geometries named Virtual Physical Model (VPM). The VPM has being developed in the Laboratory of Heat and Mass Transfer and Fluid Dynamics (LTCM). The Immersed Boundary method uses two independent domains for the solution of flows over complex geometries, namely, an Eulerian and a Lagrangian domains. The Eulerian domain used in the present work is a Cartesian mesh representing the flow field, where the Navier-Stokes equations are discretized using finite volume method over a non-uniform mesh. The time and space derivatives were approximated by a second-order scheme. The Lagrangian domain, used to locate the solid/fluid interface, is discretized by an unstructured mesh composed by triangles. The in-house parallel code runs on a Beowulf-class cluster, a viable and reliable alternative to solve highly computational demanding tasks. The three-dimensional flow over mounted cubes was simulated to capture and study horseshoes-type vortices. The results obtained present a good agreement with literature, and help understand the generation and development of such type of vortices.*

Keywords: *Immersed Boundary Method, Virtual Physical Model, Flow past Bluff Bodies*

1. INTRODUCTION

The flow over complex geometries is present in most applications of fluid mechanics in engineering. However, the numerical simulation of such flows requires sophisticated algorithms and, very often, high computational costs. In the present work the Immersed Boundary method is used as an efficient alternative to simulate the flow over complex geometries, namely, the flow around a surface-mounted cube. An in-house parallel code running on a Beowulf-class cluster is used. In Immersed Boundary (IB) methods the presence of a solid or a gaseous interface inside a flow can be simulated by adding an extra term into the discretized Navier-Stokes equations. That contribution acts as a body force in the source term component. The way such force component is evaluated differentiates the Immerzed Boundary methodologies among them. Furthermore, an important characteristic presented by IB methodologies is that the immersed obstacle, that is the solid/fluid interface, can be represented by a Lagrangian mesh while the flow domain can be discretized by an Eulerian grid such as Cartesian or cylindrical. Some IB methods also require an interpolation/distribution procedure that promotes the transfer of information back and forth between the domains. This domain independence allows one to easily apply to the immersed body displacement and/or deformation relative to the flow grid. The development of the Immersed Boundary method is credited to Charles Peskin and his collaborators when devising a methodology to simulate the blood flow through cardiac valves. Accordingly to Peskin's work (Peskin, 1977), the source of the aforementioned force term was due to the rate of deformation of the elastic fluid/solid boundary. The constitutive points of the boundary were tied by elastic membranes. More recently, Lima e Silva (Lima e Silva et al, 2003) proposed a model that evaluates the force field by applying the balance of the momentum equation, discretized by a three points stencil frame. The proposal is similar to Mohd-Yusof's (Mohd-Yusof's,1997) work but using a more simplified interpolation scheme which requires less computing resources. Since the model applies the no-slip condition at the body wall indirectly - via balance of momentum equation of the adjacent flow - the model has been named Virtual Physical Model (VPM) (Lima e Silva et al, 2003). The present work describes an application of the VPM extended to three-dimensional domains as part of the work of Campregher (Campregher, 2005).

2. MATHEMATICAL AND NUMERICAL MODELING

The Immersed Boundary method uses two distinct domains to evaluate the flow around a complex geometry. An Eulerian grid is used to discretize the fluid domain for the solution of the flow field. The Lagrangian domain, for its

turn, is used to represent the fluid/fluid or fluid/solid interface. Thus, the solution of the flow field can be tackled by using a more simple grid, e.g. Cartesian grid, whereas the complex geometry respresented by the fluid/solid interface is discretized by a versatile Lagrangian set of points. As previously mentioned, that Eulerian/Lagrangian representation is the great advantage in favour of Immersed Boundary methods, especially true for fluid-structure interaction problems where the structure undergoes deformation and/or displacement. The Virtual Physical Model (Lima e Silva et al, 2003) then acts as the coupling algorithm between the Eulerian and Lagrangian domains. The methodology and both Eulerian and Cartesian domains are detailed in following sections.

2.1 The Eulerian Domain

The Cartesian domain is discretized by Finite Volume method over a structured non-uniform mesh. The flow is considered incompressible and isothermal. The integral form of the Navier-Stokes for such assumptions becomes:

$$\frac{\partial}{\partial t}\int_{\Omega}\rho\phi d\Omega + \int_{S}\rho\phi v\cdot n\,dS = \int_{S}\Gamma\nabla\phi\cdot n\,dS + \int_{\Omega}q_{\phi}d\Omega, \tag{1}$$

where ϕ is a property being transported, q_ϕ is the term of generation or destruction of ϕ, and Γ^ϕ, is the diffusivity of ϕ. The time derivative is approximated by a second-order three-time level (Ferziger and Peric, 2002), and the spatial derivatives by the Central-Difference Scheme. The pressure-velocity coupling is done by the SIMPLEC method (Van Doormal and Raithby, 1984), and no relaxation is applied to the solution of the discretized momentum equations. The flow variables are placed in a co-located arrangement, and the Rhie-Chow (Rhie-Chow, 1983) interpolation method is used to avoid numerical oscillations due to pressure checkerboard fields. The linear systems originated from the discretization of velocity components and pressure correction equations discretization are solved, respectively, using SOR and SIP algorithm. The time and space integration of Eq. (2) over an elementary volume (Fig. 1), after some mathematical arrangements leads to the following equation:

$$\begin{aligned}&\left(\tfrac{3\phi_p^n-4\phi_p^{n-1}+\phi_p^{n-2}}{2\Delta t}\right)\Delta x\Delta y\Delta z + \left(\rho_e u_e\phi_e-\rho_w u_w\phi_w\right)^n\Delta y\Delta z + \left(\rho_n u_n\phi_n-\rho_s u_s\phi_s\right)^n\Delta x\Delta z+\\ &\left(\rho_t u_t\phi_t-\rho_b u_b\phi_b\right)^n\Delta x\Delta y = \left[\left(\Gamma^\phi\tfrac{\partial\phi}{\partial x}\right)_e-\left(\Gamma^\phi\tfrac{\partial\phi}{\partial x}\right)_w\right]^n\Delta y\Delta z+\left[\left(\Gamma^\phi\tfrac{\partial\phi}{\partial y}\right)_n-\left(\Gamma^\phi\tfrac{\partial\phi}{\partial y}\right)_s\right]^n\Delta x\Delta z+\\ &\left[\left(\Gamma^\phi\tfrac{\partial\phi}{\partial z}\right)_t-\left(\Gamma^\phi\tfrac{\partial\phi}{\partial z}\right)_b\right]^n\Delta x\Delta y + q_\phi\Delta x\Delta y\Delta z\end{aligned} \tag{2}$$

The first term of the left-hand side of the Eq.(2) represents the discretization of the transient term by the three-time level scheme (Muzaferija and Peric, 1997). This scheme is second order accurate in time.

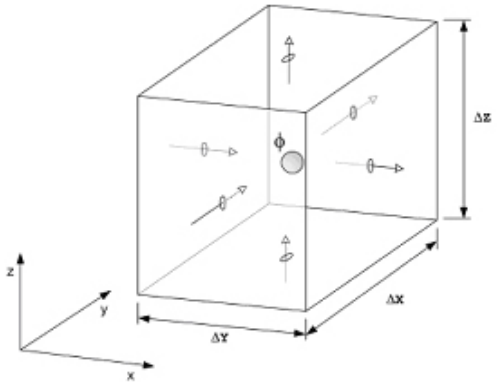

Figure 1. Elementary control volume, with variable ϕ placed on centroid.

2.2 The Lagrangian domain

The Lagrangian approach to analyze the movement of a particle constitutes of placing a system of coordinates at the particle of interest. In other words, the system of coordinates moves through the flow following the particle. Thus, at each time step the particle maintains its own system of coordinates relatively to a global system of coordinates. In the Virtual Physical model the geometry to be simulated is characterized by a Lagrangian set of points, as seen in Fig. (2). This methodology permits to take advantage of the Lagrangian approximations like the ability to simulate moving bodies by just applying translation operations to the set of points.

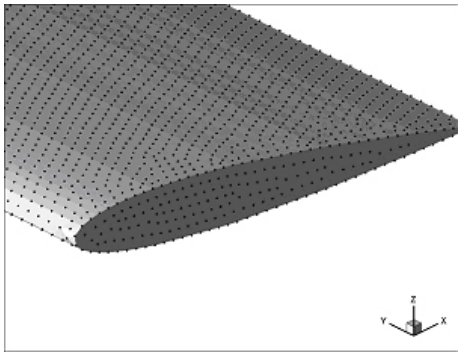

Figure 2. The surface of an airfoil NACA-0012 characterized by Lagrangian points (Vedovoto et al, 2006).

The main characteristic of Immersed Boundary method is to simulate the presence of a fluid/solid or fluid/fluid interface inside a flow by adding a source term of force $\vec{f}$ to the Navier-Stokes equations. In Fig. (3) an arbitrary Lagrangian point k is shown with coordinates $\vec{x}_k$, as well as an elementary volume of fluid with coordinates $\vec{x}$. The evaluation of $\vec{f}$ differentiates the IB methods among them.

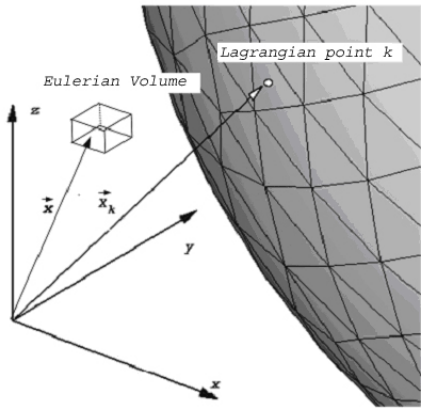

Figure 3. Schematic drawing of an arbitrary point k over a surface, placed on $\vec{x}_k$, and a element of fluid positioned in $\vec{x}$.

In the Virtual Physical Model, the Lagrangian force is obtained out of a balance of momentum over a particle k, placed at $\vec{x}_k$. The particle also has properties pressure p_k, and velocity $\vec{V}_k$. Thus, the force can be evaluated as:

$$\vec{F}_k = \frac{\partial\left(\rho\,\vec{V}_k\right)}{\partial t} + \vec{\nabla}\cdot\left(\rho\,\vec{V}_k\,\vec{V}_k\right) - \mu\nabla^2\vec{V}_k + \vec{\nabla}p_k. \tag{3}$$

The Eq. (3) can be interpreted as the necessary force so that a particle of fluid immediately adjacent to the Lagrangian point k attains the same velocity of that point, that is, one imposes a no-slip condition between the fluid and the walls of the immersed body. Each term of the Eq. (3) has its own contribution to the overall force and can be analyzed as follows. The first and second terms (the transient term) on the left-hand side are responsible, respectively, by the acceleration force ($\vec{F}_{acc}$) and inertial force ($\vec{F}_{inert}$). On the right-hand side, the terms accounts for the viscous ($\vec{F}_{visc}$) and pressure forces ($\vec{F}_{press}$), respectively. More details about the model and the evaluation of each term can be found in Lima e Silva, (Lima e Silva et al, 2003), and Campregher (2005). The properties of the flow in the Eulerian mesh must then be interpolated to the Lagrangian mesh to calculate the Lagrangian forces. Once evaluated, the Lagrangian forces must be transferred back to the Eulerian domain and inserted into the source-term of the discretized Navier-Stokes equation. The connection between Lagrangian and Eulerian domains is promoted by the force distribution procedure.

2.2.1 The Virtual Physical Model

The discretization of Eq (3) is done by setting a three-dimensional reference axis, with origin placed at the point k , as depicted in Fig (4). A Lagrangian polynomial is then used to obtain the space derivatives along each coordinate direction. Let m be a number of points employed to construct a polynomial interpolation of order $m-1$. Thus, the value of a

property ϕ along the i direction, at any point p, is given by:

$$\phi_i(p) = \sum_m \psi_m(p)\,\phi_m, \tag{4}$$

where,

$$\psi_m(p)_i = \prod_{n,n\neq m} \left[\frac{x_i(p) - x_i(n)}{x_i(p) - x_i(n)}\right]. \tag{5}$$

Substituting the m points, according to the stencil in Fig (4), the ϕ property value along the x axis (where k, k_1 and k_2 points lay) can be obtained as:

$$\phi_p = \left[\frac{(x_p - x_{k1})(x_p - x_{k2})}{(x_k - x_{k1})(x_k - x_{k2})}\right]\phi_k + \left[\frac{(x_p - x_k)(x_p - x_{k2})}{(x_{k1} - x_k)(x_{k1} - x_{k2})}\right]\phi_{k1} + \left[\frac{(x_p - x_k)(x_p - x_{k1})}{(x_{k2} - x_k)(x_{k2} - x_{k1})}\right]\phi_{k2}. \tag{6}$$

Deriving Eq (6) with respect to x component one has:

$$\frac{\partial\phi_p}{\partial x} = \left[\frac{(x_p - x_{k1}) + (x_p - x_{k2})}{(x_k - x_{k1})(x_k - x_{k2})}\right]\phi_k + \left[\frac{(x_p - x_k) + (x_p - x_{k2})}{(x_{k1} - x_k)(x_{k1} - x_{k2})}\right]\phi_{k1} + \left[\frac{(x_p - x_k) + (x_p - x_{k1})}{(x_{k2} - x_k)(x_{k2} - x_{k1})}\right]\phi_{k2}, \tag{7}$$

and the second derivative results:

$$\frac{\partial^2\phi_p}{\partial x^2} = \left[\frac{2\phi_k}{(x_k - x_{k1})(x_k - x_{k2})}\right] + \left[\frac{2\phi_{k1}}{(x_{k1} - x_k)(x_{k1} - x_{k2})}\right] + \left[\frac{2\phi_{k2}}{(x_{k2} - x_k)(x_{k2} - x_{k1})}\right]. \tag{8}$$

From the equations above, it is possible to obtain every spatial derivative needed in Eq (3) by substituting the point p of interest and the working variable ϕ.

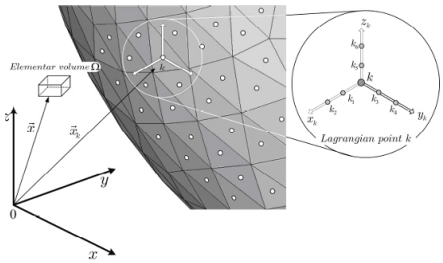

Figure 4. Position of the Lagrangian point $\vec{x}_k$.

A detailed view of a triangular element is shown in Fig (5). The sides of the element are formed by the line segments S_1, S_2, and S_3, connecting the vertex points P_1, P_2 and P_3. Thus, one has $S_1 = \overline{P_2P_1}$, $S_2 = \overline{P_2P_3}$, and $S_3 = \overline{P_3P_1}$. The ΔA_k is the triangular element surface area, evaluated as:

$$\Delta A_k = \sqrt{S(S - S_1)(S - S_2)(S - S_3)} \tag{9}$$

where $S = (1/2)(S_1 + S_2 + S_3)$. The ΔS_k is the average length of the triangle sides. It worth noting that each of those geometric properties are associated to the Lagrangian point k.

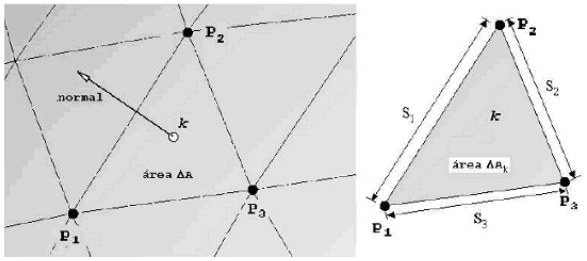

Figure 5. Detailed view of a triangular element.

2.2.2 The distribution procedure

The Lagrangian force term $\vec{F}$, calculated at a Lagrangian point (denoted by k) is then distributed to the Eulerian domain by means of the Dirac's delta function. In a N-dimensional domain this function is defined as:

$$\vec{f}(\vec{x}) = \int_{R^n} \delta(\vec{x} - \vec{x}_k)\vec{F}(\vec{x}_k)d^n\vec{x}_k \tag{10}$$

Applying the Eq. (10) to a volume V of the Lagrangian domain,

$$\vec{f}(\vec{x}) = \int_{\Omega_n} \vec{F}(\vec{x}_k)\delta(\vec{x} - \vec{x}_k)d\vec{x}_k \ . \tag{11}$$

and δ function has the following property:

$$\int_{R^n} \delta(\vec{x} - \vec{x}_k)d\vec{x} = \begin{cases} 1 & if\ \vec{x}_k \in V \\ 0 & if\ \vec{x}_k \notin V \end{cases} , \tag{12}$$

where $V \in \Omega$. This function acts as the core of a transformed integral (centered in $\vec{x}_k$), which promotes the transposition between the Lagrangian and Eulerian domains (Griffith and Peskin, 2005). For the three-dimensional version of the Virtual Physical Model, the Lagrangian force field $\vec{F}_i$ is distributed over the Eulerian mesh using Eq (13):

$$f_i = \sum F_i D_i \Delta A_k \Delta S_k. \tag{13}$$

The distribution function D_i is evaluated as:

$$D_i\left(x_k\right) = \prod_i \left\{ \frac{\varphi\left[\left(x_k - x_i\right)/\Delta x_i\right]}{\Delta x_i} \right\} \tag{14}$$

where the φ function is defined as:

$$\varphi\left(r\right) = \begin{cases} \tilde{\varphi}\left(r\right) & if\ \ \|r\| < 1 \\ \frac{1}{2} - \tilde{\varphi}\left(2 - r\right) & if\ 1 < \ \|r\| < 2 \\ 0 & if\ \ \|r\| > 2 \end{cases} , \tag{15}$$

$$\tilde{\varphi}\left(r\right) = \frac{3 - 2\left\|r\right\| + \sqrt{1 - 4\left\|r\right\| + 4\left\|r\right\|^2}}{8}. \tag{16}$$

The Distribution function is divided by a volume unit, that cancels out by multiplying by a characteristic area (ΔA_k) and length ΔS_k. Thus, the remainder is a force density that is integrated over the volume Ω.

The interface solid/fluid is a halo represented by an indicator function I_i, built from:

$$\nabla^2 I_i = \nabla G_i, \tag{17}$$

where the G function is defined as:

$$G_i = \sum D_i \vec{n}_k \Delta A_k, \tag{18}$$

and the $\vec{n}_k$ is the normal vector at the Lagrangian point k. After the discretization of the Eq. (17), the algebraic equation system is evaluated by the MSI algorithm (Schneider and Zedan, 1981), a variation of the SIP algorithm. By analyzing the Eq. (18), one can see that if the geometry is inserted into a non-uniform grid region, the interfacial region may become deformed, i.e., the geometry shell shape would be misrepresented. Briefly describing, the force field evaluation procedure in the Virtual Physical Model can be stated as:

(1) With the flow field solved, the velocity components and the pressure are transferred, using the interpolation function given by Eq. (18), to the nearest Lagrangian points (k, k_1...k_6) depicted in Fig. (4);

(2) Once having u_i and p_i, one evaluates the Lagrangian force field, F_i, using Eq. (3);

(3) The Eulerian force field components are then calculated, taking into account the force at each Lagrangian point k via Eq. (13);

(4) One advances in time;

(5) The Eulerian force field is inserted into the source-term of the Navier-Stokes equations - Eq. (1);

(6) A new flow field is obtained and the procedure repeats.

3. PARALLEL PROGRAMMING APPROACH

One of the greatest concerns involving the solution of complex problems in Computational Fluid Dynamics is the computational cost. Thus, an in-house Beowulf cluster turns out to be very a viable solution due to its comparatively low cost when comparing to the supercomputers. Moreover, such clusters have good scalability, that is, it is possible to increase the cluster computational power by appending more processors to the network. The cheaper assembly is ensured by employing off the shelf hardwares and open source softwares, freely downloaded from internet. Any group of ordinary machines connected by a local network may constitute a Beowulf cluster. The cluster used in the present work is a five CPUs with following configurations: mother-board Intel 865PERL , processor Pentium4 2.8GHz, 1548 MB DDR RAM, and 80 GB IDE hard drive. The main difference between the master and slave nodes is that the former has a Radeon 9200 128MB DDR AGP8x video card, whereas the latter have a Geforce 64MB AGP4x. The post-processing tasks are done by master node. All machines are connected by a Gigabit network via 3COMő 16 port switch. The data exchange among processors is managed by the MPI (Message Passage Interface) library, more specifically the MPICH (MPI CHameleon) version. The MPI has been chosen, mainly, due to its better performance on clusters of homogeneous machines. Furthermore, the MPI library has more than 120 functions permitting to write very efficient codes and, also, it is constantly updated by the MPI community. The computational domain is split into four sub-domains with the Lagrangian mesh entirely in one of them, since it is not parallelized yet. Furthermore, as described above, it is imperative to use uniform spaced grids around the immersed geometry region. However, the rest of the Eulerian domain was discretized in a non-uniform mesh to lessen computational costs.

4. RESULTS AND DISCUSSION

Although a surface-mounted cube is a geometrically simple problem, the flow around such geometry might generate highly complex coherent structures, like horseshoes vortices and hairpin vortices. Also, the surface-mounted cube was chosen as a test case due to verify the robustness of the solver. To reduce the computational costs of generating the indicator function, a computational box surrounding the immersed boundary is inserted, as described in Lima and Silva, (2002). The box should be large enough to contain all interpolation points depicted in Fig. 4. In the same picture, it is possible to note that the Lagrangian coordinate axis at each point is independent and parallel to the Cartesian coordenate axis. Such configuration required some changes in the numerical code for the present work. Basically, changes were done to avoid the presence of interpolation points outside the domain when the geometry is placed close to the flow boundary, making the simulations impracticable. In cases where those adjusts were necessary the direction of the Lagrangian axis - where the auxiliary points lay - was turned inward. In these cases the new direction is the opposite of the original one, ensuring that no point is placed outside the Eulerian domain. The Fig. 6 shows the Eulerian mesh (Cartesian), the computational box (bold black line), and the cube computational mesh (triangular elements type). It is also possible to see in Fig. 6 the directions of the original vector for the interpolations points along the z direction (dashed arrow), and the vector with the new direction (red arrow).

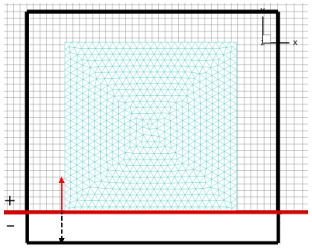

Figure 6. Drawing of the scheme of directions for the vectors used in the interpolations.

The changes in the direction of the vectors have not represented any problem for immersed boundary method and the results obtained after such procedure were physically consistent. In the case of the surface-mounted cube another alteration was needed, namely, a $adhoc$ constant was applied to acceleration term of the evaluation of Lagrangian force. Thus, the acceleration force is given by:

$$\vec{F}_{acc} = \frac{\rho}{C}\left(\frac{-U_{ki}}{\Delta t}\right). \tag{19}$$

where C is the $adhoc$ constant = 0.1, U_{ki} is the velocity of a Lagrangian point k, and Δt is the time step.

The results obtained in the present work are compared against the work of Hwang and Yang (2004), for Reynolds numbers of 350 and 1.000. The dimensions of the computational domain for both works are the same. The Eulerian domain is 1.2 x 0.7 x 0.2 m, discretized in a mesh composed by 196 x 136 x 79 volumes. Also, as aforementioned, the

computational domain is divided into four processors. The boundary conditions for the Eulerian domain are non-slip wall at $z = 0$, and free surface at $z = z_{max}$, $y = 0$ and $y = y_{max}$. By the definition of VPM, the immersed boundary imposes non-slip condition at the cube walls. The Fig. 7 shows the isosurfaces of Q obtained for the simulation of the flow at Reynolds number of 1.000 by Hwang e Yan, (2004) (on left hand side), and obtained in the present work. It is possible to note the good qualitatively agreement between the results.

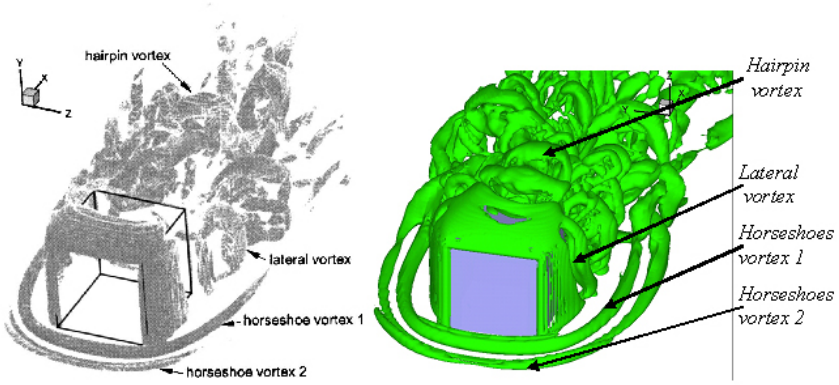

Figure 7. Isosurfaces of Q obtained by Hwang e Yang,(2004) (left), and the present work (right) at $Re = 1.000$.

Another great similarity occurs between Fig. 8 (obtained by Hwang e Yang (2004)) and Fig. 9.(obtained in the present work). In both figures the streamlines are shown in a plane close to the wall where the cube is mounted on.

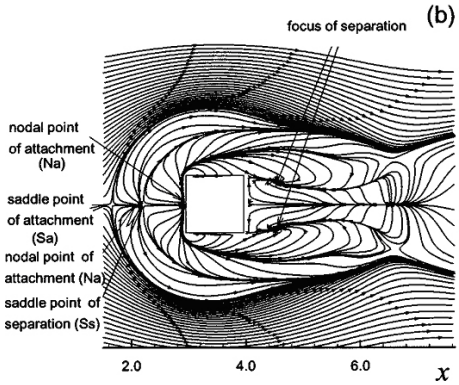

Figure 8. Streamlines at $Re = 350$ xz plane, $x = 0,0053m$, (Hwang e Yang (2004)).

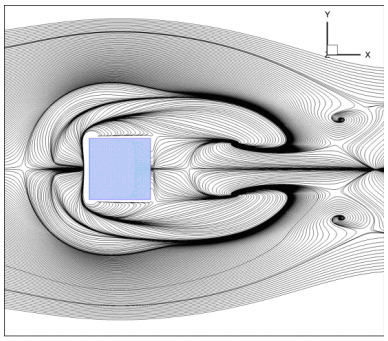

Figure 9. Streamlines at $Re = 350$ xy plane, $z = 0,001m$, (present work).

The 3D streamlines in Figure 10 show clearly the formation of the horseshoes vortices upstream the cube.

Figure 11 shows isosurfaces of $Q = 75$, colored by u velocity ($Re = 1.000$).

A quantitative comparison is made between flows at Reynolds number 350 and 1.000. In Fig. 12, one can note three pairs of curves of temporal evolution. These curves represent, respectively, the drag, side, and lift coefficients, for both

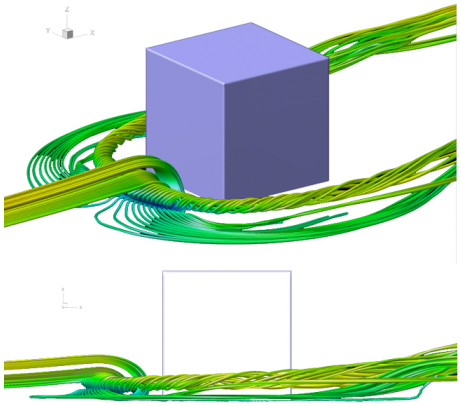

Figure 10. 3D Streamlines showing the formation of horseshoes-type vortices ($Re = 1.000$) .

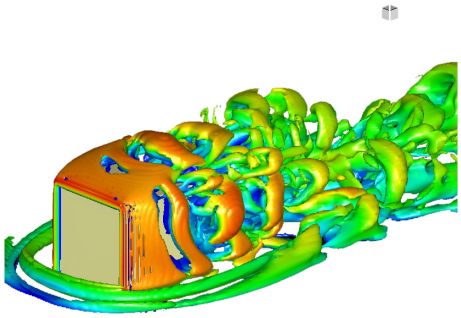

Figure 11. Isosurfaces of $Q = 75$, ($Re = 1.000$).

flows at $Re = 350$ and $Re = 1.000$. Also, there is a slightly increment in the value of the drag coefficient at Reynolds number 350, which is expected physically. There is no noticeable differences for the lift and side coefficients, once both curves oscillate about the same value (0.4 for the lift coefficient, and 0.0 for the side coefficient).

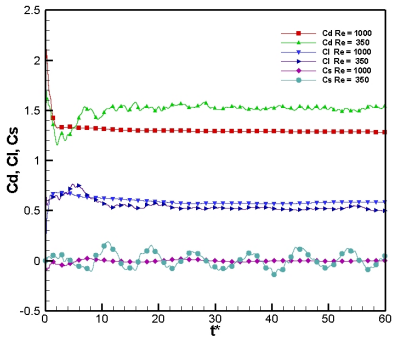

Figure 12. Temporal evolution of quantitative parameters for the flow over a surface-mounted cube.

5. CONCLUSION

In the present work, which represents an extension of Campregher's work (Campregher, (2005)), the authors intended to present a more complex application of the Virtual Physical Model. The flow around surface-mounted cube at $Re = 350$ and $Re = 1.000$ was chosen as a test case to identify and characterize the generation and the decay of coherent structures like horseshoes vortices and hairpin vortices. It was done successfully and the results presented a good agreement with literature (Hwang and Yang, (2004)). However, further investigation about the influence of high Reynolds number still

has to be done. The Immersed Boundary method has demonstrated great capability in dealing with complex geometries. Firstly because the flow field is discretized using a geometrically simple Cartesian mesh. Secondly, it is very simple to discretize the complex geometry using a Lagrangian mesh. Those features represent important advantage when compared with other methodologies for the solution of Fluid-Structure Interaction problems.

6. ACKNOWLEDGEMENTS

The authors would like to thank CNPq and CAPES for the financial support.

7. REFERENCES

Campregher, Rubens, 2005, "Modelagem Matemática tridimensional para problemas de interação fluido-estrutura",doctoral thesis, Uberlândia

Ferziger J and Peric M.,2002, Computational methods for fluid dynamics 3th ed., Springer-Verlag, New-York, USA.

Griffith, B. and Peskin, C., 2005, "On the order of accuracy of the immersed boundary method: Higher order convergence rates for sufficiently smooth problems.", Journal of Computational Physics 208, 75-105. Mechanical Sciences, Vol.19, No. 3, pp. 332-340.

Hwang, J. and Yang, K., 2004, "Numerical study of vortical structures around wall-mounted cubic obstacle in channel flow", Physics of Fluids, Vol.16, No. 7, 2382-2394.

Lima e Silva A.L.F., 2002, "Desenvolvimento e implementação de uma nova metodologia de modelagem de escoamentos sobre geometrias complexas: método da fronteira imersa com modelo físico virtual",doctoral thesis, Uberlândia

Lima e Silva A.L.F., Silveira-Neto, A., and Damasceno, J.J.R, 2003, "Numerical simulation of two dimensional flows over a circular cylinder using the immersed boundary method.", J. Comp. Phys. 189, 351.

Mohd-Yusof, J., 1997, "Combined immersed boudaries/B-splines methods for simulations in complex geometries", CTR Annual Research Briefs, NASA Ames/Stanford University.

Muzaferija, S. and Peric, M., 1997, "Computational of free-surface flows using the Finite-Volume method and moving grids", Numerical Heat Transfer, Part B 32, 369-384.

Peskin C.S., 1977, "Numerical analysis of the blood flow in the heart", J. Comp. Phys. 25, 220.

Rhie C. and Chow W., 1983, "Numerical study of turbulent flow past an airfoil with trailing edge separation", AIAA Journal 21, 1525.

Schneider G.E. and Zedan M., 1981, "A modified strongly implicit procedure for the numerical solution of field problems", Numerical Heat Transfer 4, 1.

Van Doormal, J. and Raithby, G., 1984, "Enhancements of the simple method for predicting incompressible fluid flows", Numerical Heat Transfer 7, 147-163.

Vedovoto, J. M., Campregher, R., Silveira Neto, A., 2006, "Mathematical modeling and numerical simulation of a three-dimensional flow over complexes geometries using the immersed boundary method", Proceedings of 11th Brazilian Congress of Congress of Thermal Sciences and Engineering - ENCIT.

8. Responsibility notice

The author(s) is (are) the only responsible for the printed material included in this paper